Rock Mech. Rock Engng. (1999) 32 (2), 81–99

Rock Mechanics and Rock Engineering

Effects of Grain Size on the Initiation and Propagation Thresholds of Stress-induced Brittle Fractures

By

E. Eberhardt[1], **B. Stimpson**[2], and **D. Stead**[3]

[1] Engineering Geology, Swiss Federal Institute of Technology (ETH), Zürich, Switzerland
[2] Department of Civil and Geological Engineering, University of Manitoba, Winnipeg, Canada
[3] Camborne School of Mines, University of Exeter, U.K.

Summary

The microstructure of rock is known to influence its strength and deformation characteristics. This paper presents the results of a laboratory investigation into the effects of grain size on the initiation and propagation thresholds of stress-induced brittle fracturing in crystalline rocks with similar mineralogical compositions, but with three different grain sizes. Strain gauge and acoustic emission measurements were used to aid in the identification and characterization of the different stages of crack development in uniaxial compression. Results indicate that grain size had only a minor effect on the stress at which new cracks initiated. Crack initiation thresholds were found to be more dependent on the strength of the constituent minerals. Grain size did have a significant effect, however, in controlling the behaviour of the cracks once they began to propagate. The evidence suggests that longer grain boundaries and larger intergranular cracks, resulting from increased grain size, provide longer paths of weakness for growing cracks to propagate along. This promoted degradation of material strength once the longer cracks began to coalesce and interact. Thus, rock strength was found to decrease with increasing grain size, not by inducing crack initiation at lower stresses, but through a process where longer cracks propagating along longer planes of weakness coalesced at lower stresses.

1. Introduction

The study of brittle fracture and its relationship to deformation and strength forms a fundamental area of research in rock mechanics and several other engineering disciplines. Fracturing is considered to be a process through which bonds are broken, and new surfaces are formed as a new or existing crack in an otherwise

intact material propagates. The initiation, propagation and coalescence of these cracks result in the degradation of material strength which eventually leads to failure. These processes have been largely studied through the application of mechanistic-derived criteria, based on the premise that fractures initiate from existing flaws acting as stress concentrators, otherwise known as Griffith's theory (Griffith, 1920; Griffith, 1924).

The practical application of these theories (e.g. Griffith's theory, linear elastic fracture mechanics) primarily involves the determination of the stress threshold at which a crack initiates and begins to propagate. Applying Griffith's theorem for an elliptical crack loaded in compression (Griffith, 1924):

$$\sigma_C \geq 8^* \sqrt{\frac{2E\alpha}{\pi c}} \tag{1}$$

where: σ_C = compressive stress required for fracture;
E = elastic or Young's modulus;
α = surface energy per unit area of the crack surfaces;
c = crack half-length;

it can be seen that the smaller the crack length, the greater the stress required for fracture initiation. Numerous studies have confirmed that the peak strength of rock decreases inversely with the square root of the grain size (Brace, 1961; Olsson, 1974; Hugman and Friedman, 1979; Fredrich et al., 1990; Wong et al., 1996; Hatzor and Palchik, 1997). In these cases, the "Griffith" crack length can be taken as being roughly proportional to the grain size.

In situ observations of tunnel performance at the Atomic Energy of Canada Limited's Underground Research Laboratory (URL) appear to agree with these findings. The structure of the Lac du Bonnet batholith, which houses the URL, is such that rock types of three different grain sizes are encountered. Referred to herein as Lac du Bonnet grey granite, granodiorite and pegmatite, these rock types represent a large variation in grain size while still falling within the International Union of Geological Sciences (IUGS) classification for granite (Read, 1994). Martin et al. (1997) report that the severity of stress-induced spalling observed following tunnel advancement at the URL was more pronounced in regions comprised predominantly of grey granite than in the finer-grained granodiorite (Fig. 1). A laboratory study, based on uniaxial compression testing, was subsequently conducted to determine the brittle fracture characteristics of the Lac du Bonnet rock types and to determine what role grain size plays in controlling their deformation and strength attributes.

2. Experimental Methodology

2.1 Grain Size and Cracks in Rock: Observations and Theory

Simmons and Richter (1976) and Kranz (1983) divide microcracks in rock into four types:

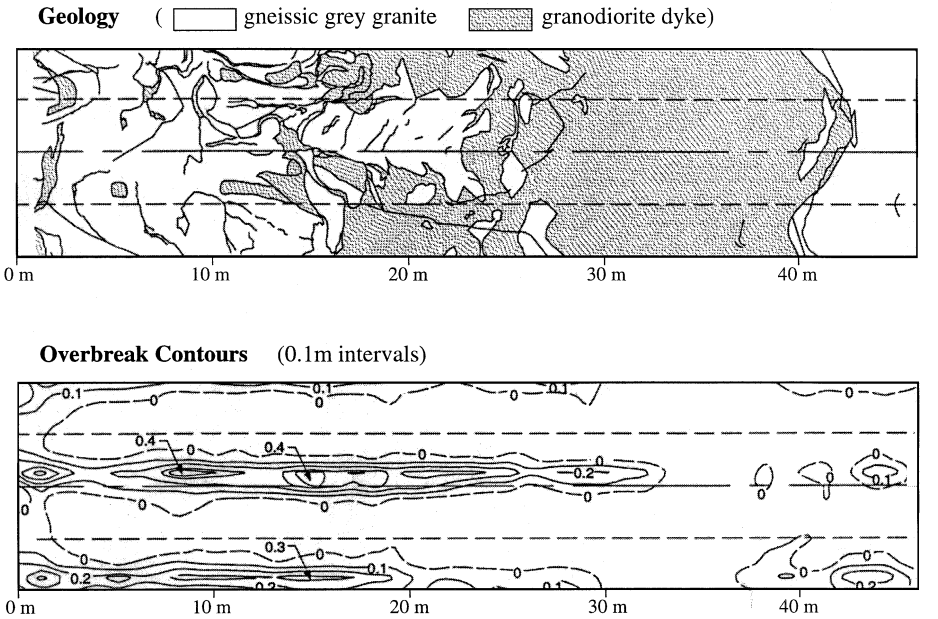

Fig. 1. Fold-out perimeter maps showing the geology and the corresponding depth of overbreak in a circular test tunnel at the URL (after Martin et al., 1997)

- grain boundary cracks (cracks associated with grain boundaries);
- intragranular cracks (cracks which lie totally within the grain and do not extend to a grain boundary);
- intergranular cracks (cracks which extend from a grain boundary crossing into the grain);
- and multigranular cracks (cracks which cross several grains and grain boundaries).

In crystalline materials, it is widely assumed that grain boundaries act as the predominant source of stress concentrating flaws and that the initial flaw lengths will be on the order of scale of the materials grain size.

Direct observations of microfractures using optical microscopes, scanning electron microscopes (SEM) or other petrographic techniques, have drawn a variety of conclusions as to which crack type constitutes the weakest plane and is therefore most prone to fracture propagation. Brace (1961) found that in the case of anhydrites, limestones and quartzites, the first detectable fracturing starts at the grain boundaries. In crystalline, igneous rock, Brace et al. (1972) determined that although grain boundaries are the preferred site of microcracks, intragranular cracks also occur in some of the weaker mineral constituents such as feldspar and biotite grains. Other studies have found that fracturing primarily occurs along grain boundaries with secondary fracturing occurring within weaker grains, either between cleavage planes or at points where harder minerals induce a point load on neighbouring, softer minerals (Wawersik and Brace, 1971; Bombolakis, 1973;

Sprunt and Brace, 1974; Mosher et al., 1975; Tapponnier and Brace, 1976; Kranz, 1979).

As previously noted, from Eq. (1), the strength of crystalline rocks should increase with decreasing crack or flaw size. Fredrich et al. (1990) also observed that the increase in crack density that would be expected with finer-grained materials can be equated to an increase in the spatial heterogeneity of the local stress field. Such heterogeneity will clearly have strong effects on the crack propagation behaviour, and may cause crack arrest at stages earlier than those predicted by Eq. (1). This effect has been demonstrated using numerical modelling techniques by Eberhardt et al. (1998a).

2.2 Detection of the Microfracturing Process Through Laboratory Measurements

Based on laboratory studies by Brace (1964) and Bieniawski (1967), the failure process of brittle rock has been broken down into the following stages:

1. crack closure;
2. linear elastic deformation;
3. crack initiation and stable crack growth;
4. volumetric strain reversal (crack damage) and unstable crack growth;
5. failure and post peak behaviour.

These stages can be identified through the analysis of axial and lateral strains measured by electric resistance strain gauges mounted on the test specimen. Crack closure, σ_{cc} in Fig. 2, occurs during the initial stages of loading when existing cracks orientated at an angle to the applied load close. During crack closure, the stress-strain response is non-linear and exhibits an increase in axial stiffness. Once the majority of existing cracks have closed, linear elastic deformation takes place. Crack initiation, σ_{ci}, represents the stress level where microfracturing begins and is marked as the point where the lateral and volumetric strain curves depart from linearity (i.e. as initiating crack faces open perpendicular to axial loading). Crack propagation can be considered as being either stable or unstable. Under stable conditions, crack propagation can be stopped by controlling the applied load. Bieniawski (1967) defines unstable crack propagation as the condition which occurs when the relationship between the applied stress and the crack length diminishes and other parameters, such as the crack growth velocity, take control of the propagation process. With reference to strain gauge measurements, the unstable crack propagation threshold has been associated with the point of reversal in the volumetric strain curve which Martin (1993) refers to as the crack damage stress threshold, σ_{cd} (Fig. 2).

Precisely establishing these thresholds through laboratory testing, however, can prove difficult, especially with respect to crack initiation. Eberhardt (1998) found that methods based on the estimate of crack volume, as described by Martin and Chandler (1994), were suspect due to their sensitivity to the elastic constants E and ν used in the calculations. It was found that the crack initiation threshold could be more accurately determined by using an approach that combined measurements of acoustic emissions with strain gauge data (these techniques are

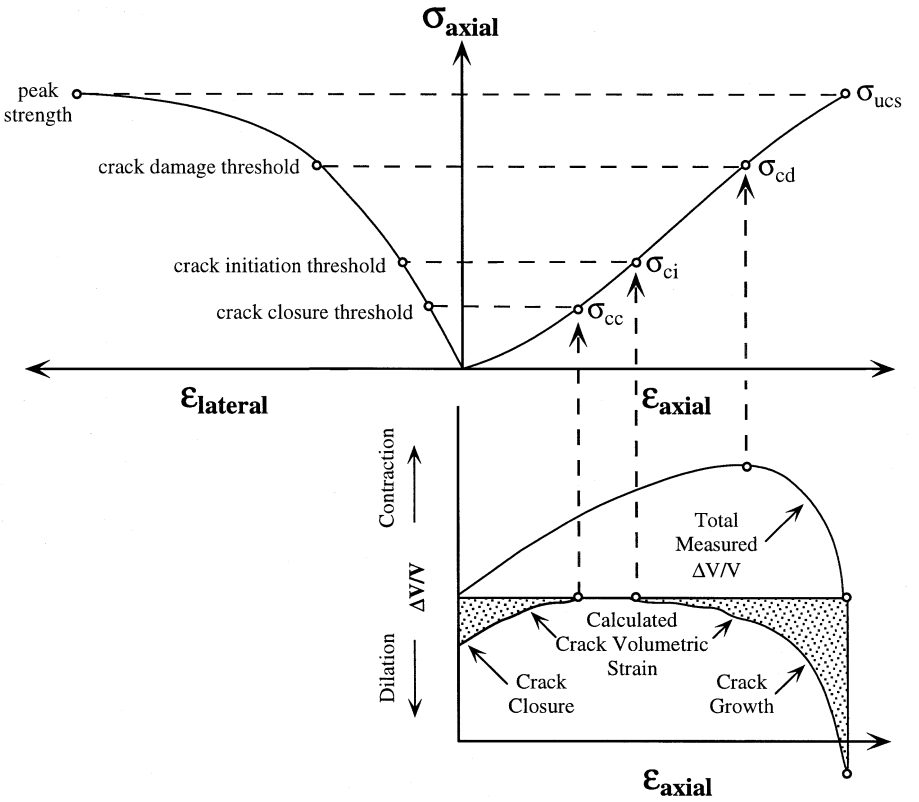

Fig. 2. Stress-strain diagram showing the stages of crack development (after Martin, 1993). Note that only the axial and lateral strains are measured; the volumetric and crack volume strains are calculated

described in detail by Eberhardt et al., 1998b). The threshold values determined by combining these two techniques, and further confirmed through measured changes in the AE event properties (Eberhardt et al., 1997) and "energy" (Eberhardt et al., 1998b), led to the identification of two additional thresholds in crack development for Lac du Bonnet pink granite. The first marks the initiation of cracking within the stronger quartz grains of the granite following the initial cracking observed in the weaker feldspar grains, and was termed the secondary crack initiation threshold, σ_{ci2}. The second marks the beginning of crack interaction and coalescence, termed the crack coalescence threshold, σ_{cs}. These methods of data analysis were subsequently applied to a variety of rock types, including Lac du Bonnet granite, Saskatchewan potash and Berea sandstone (Eberhardt, 1998). Due to the large contrast in material behaviour exhibited by these different rock types, a rigorous methodology was defined to help in establishing each of the different thresholds of crack development (Table 1). It should therefore be noted that the crack thresholds shown in the ensuing plots are not solely determined through the plot in which they are depicted, but through a combination of the different analysis techniques utilized.

Table 1. Methodology used to establish the different thresholds of crack development (Note: stiffness curves are briefly defined in Section 3.2 and are described in detail in Eberhardt et al., 1998b)

Crack Threshold	Description
Crack closure	The crack closure threshold is established using the axial stiffness curve. The threshold value is determined as the point where the axial stiffness curve shifts from incrementally increasing values (i.e. non-linear behaviour) to constant values (i.e. linear behaviour). Linear axial strain behaviour is therefore used as an indicator that preferentially aligned cracks are closed.
Crack initiation	The crack initiation threshold is based on several criteria. The primary criterion involves picking the approximate interval in which the AE event count first rises above the background level of detected events. The exact value within this interval is determined as the point in the AE event count rate and "energy" rate where values begin to significantly increase. This point is checked against the first large break from linear behaviour in the volumetric stiffness curve.
Secondary cracking	The secondary cracking threshold is taken as the first significant increase in the AE event rate following crack initiation, which in turn, coincides with the continuous detection of AE activity. Furthermore, this point can be correlated with large increases in the event "energy" rate and notable breaks in the volumetric stiffness plot.
Crack coalescence	Crack coalescence is taken from the approximate interval in which the axial stiffness curve departs from linear behaviour (i.e. as an element of non-linear axial displacement is detected in the crack propagation process). This point is checked against large irregularities in the volumetric stiffness curve. In addition, changes in the AE event rate and the different event properties may coincide with this point.
Crack damage	The crack damage threshold is taken as the point in the volumetric stiffness curve where values change from positive to negative, thereby marking the reversal of the volumetric strain curve.

3. Laboratory Testing of Grain Size Effects

As previously noted, the structure of the Lac du Bonnet batholith is such that rock types of three different grain sizes, but with similar mineralogical compositions, are encountered. Test samples of grey granite, granodiorite and pegmatite, shown in Fig. 3, were obtained from core retrieved from the 240 m level of the URL, ensuring that each rock type had been exposed to similar *in situ* stress and sampling conditions. The grey granite is homogeneous and equigranulaur, although some samples were found to be slightly porphyritic with moderately larger feldspar phenocrysts. The average grain size was approximately 3 mm. Interspersed with the grey granite of the URL, primarily below 200 m, are granodiorite dykes which are similar in mineralogy to the grey granite, with the exception that the granodiorite has slightly less feldspar and more biotite. The granodiorite is fine-grained and relatively equigranular with an average grain size of 1 mm. Descriptions of the mineralogy and grain sizes for these two rock types are given in Table 2. The third rock type tested appears on the 240 m level as pegmatitic granite dykes. This pegmatite is large grained and inequigranular with large phenocrysts of feldspar. Grain sizes range from 10 to 40 mm with an average of about 20 mm.

Cylindrical samples, 61 mm in diameter, were prepared for testing at the University of Saskatchewan's Rock Mechanics Laboratory according to ASTM standards with length to diameter ratios of approximately 2.25. These samples

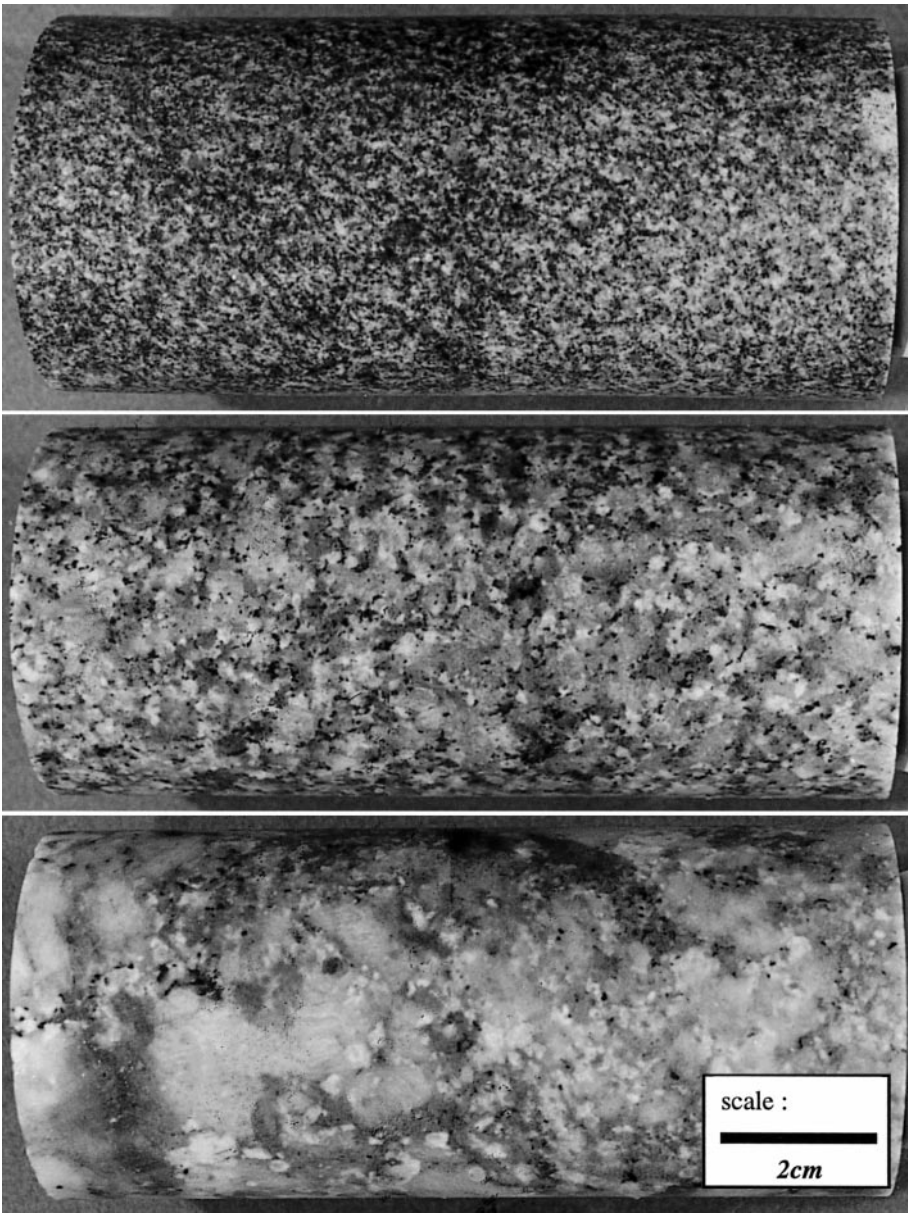

Fig. 3. Test samples from the 240 m level of the URL showing varying grain size: granodiorite (top), grey granite (middle), and pegmatite (bottom)

were instrumented with six electric resistance strain gauges (3 axial and 3 lateral at 60° intervals, 12.7 mm in length, with a 5% strain limit) and four 175 kHz resonant frequency, piezoelectric AE transducers. Uniaxial loading was applied to the samples at a constant rate of 0.25 MPa/s so that failure occurred between 5 and

Table 2. Composition and average grain sizes for URL granite and granodiorite (after Read, 1994)

Rock type	K-Feldspar		Plagioclase		Quartz		Biotite	
	mineral (%)	grain size (mm)	mineral (%)	grain size (mm)	mineral (%)	grain size (mm)	mineral (%)	grain size (mm)
Granite	45	3.7	20	3.1	30	1.8	5	0.9
Granodiorite	35	1.0	25	1.1	30	0.7	10	0.6

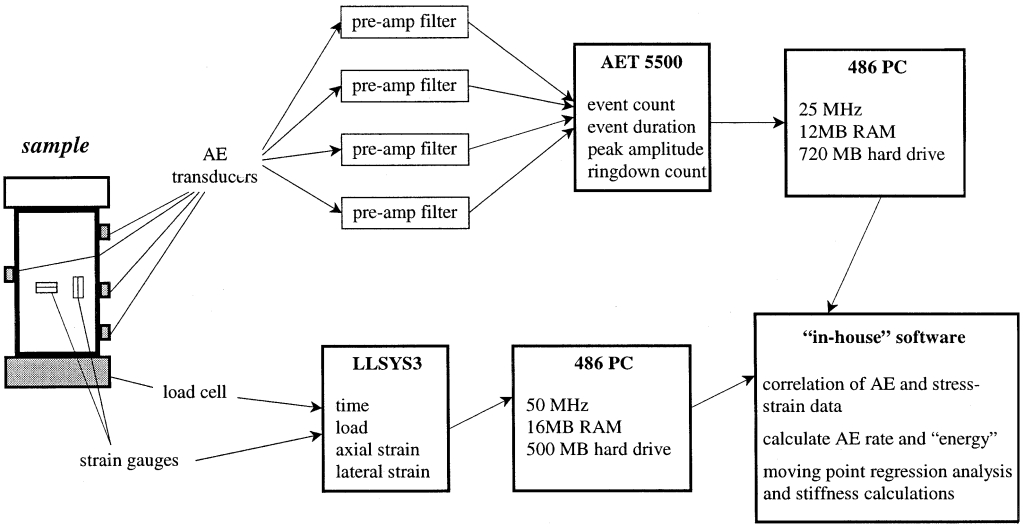

Fig. 4. Schematic of strain gauge and acoustic emission instrumentation, and data collection systems

10 minutes, as recommended by the ISRM (Brown, 1981). Applied loads and the resulting strains were recorded, using an automatic data acquisition system, sampling at an average rate of 2–3 readings per second, thereby overcoming any deficiencies in data resolution. The AE monitoring system consisted of a bandpass filter with a frequency range of 125 kHz to 1 MHz and a pre-amplifier with 40 dB total gain and a dynamic range of 85 dB. The AE data was recorded with an AET 5500 monitoring system using a threshold value of 0.1 V. A schematic of the system used is provided in Fig. 4. Prior to testing, compressional and shear wave velocities were also measured parallel to the sample axis.

3.1 Density and Acoustic Velocity Results

Although the samples are similar in mineralogical composition, the variation in grain size results in differing densities and acoustic velocities. Density was found to decrease with increasing grain size, and compressional (P-wave, or V_P) and shear

Table 3. Summary of density and acoustic velocity values for the 240 m level URL samples (standard deviation in parentheses)

Material parameter		Granodiorite	Grey granite	Pegmatite
Samples tested		5	5	5
Density	ρ (g/cm^3)	2.66 ($\pm$0.00)	2.62 ($\pm$0.01)	2.59 ($\pm$0.02)
Acoustic velocity	V_P (m/s)	5240 ($\pm$70)	4445 ($\pm$295)	5295 ($\pm$545)
	V_S (m/s)	3245 ($\pm$60)	2905 ($\pm$85)	3025 ($\pm$125)
	V_P/V_S	1.61	1.53	1.75

Table 4. Average elastic constants for the 240 m level URL samples (standard deviation in parentheses)

Material parameter	Granodiorite	Grey granite	Pegmatite
Samples tested	5	5	5
Young's modulus, E_{avg} (GPa)	67.2 ($\pm$3.5)	63.8 ($\pm$2.2)	60.1 ($\pm$1.7)
Tangent modulus, E_T (GPa)	69.4 ($\pm$1.3)	60.3 ($\pm$1.1)	57.7 ($\pm$3.0)
Secant modulus, E_S (GPa)	66.8 ($\pm$0.9)	49.7 ($\pm$1.9)	51.6 ($\pm$2.0)
Poisson's ratio, v_{avg}	0.30 ($\pm$0.03)	0.33 ($\pm$0.04)	0.29 ($\pm$0.07)

(S-wave, or V_S) velocities for the grey granite samples were found to be approximately 15% lower than those for the finer-grained granodiorite (Table 3). However, the pegmatite, which has the lowest density of the three rock types, had velocities similar to those of the granodiorite. These velocities can be attributed to the large crystals found in the pegmatite, as can the increased standard deviation seen in the test results (Table 3). Larger crystals mean fewer grain boundaries within a given volume, which act to reduce the velocity of the acoustic pulse. For example, acoustic velocities of 6240 m/s (V_P) and 3180 m/s (V_S) were measured in one of the pegmatite samples, which contained two large feldspar crystals measuring over 40 mm in diameter and constituting nearly half of the sample. The P-wave velocity for this sample was approximately the same as that given by Goodman (1989) for a single crystal of the mineral plagioclase feldspar ($V_P = 6250$ m/s). Thus, in some cases, a few mineral grains might have a dominant effect on the physical properties of the test sample.

3.2 Grain Size Dependent Deformation and Fracture Characteristics

Young's modulus, as measured over the linear portion of the stress strain curve, was found to decrease with increased grain size. Average values for the grey granite and pegmatite were found to be 5% and 11% lower, respectively, than those for the granodiorite (Table 4). These results suggest that the degree of intercrystalline deformation, plastic flow, dislocation glide and other similar elasto-plastic sliding mechanisms, slightly increases with increasing grain size. Similar observations, but with significantly higher strains, were made by Fredrich et al. (1990) for marble where an association was found between grain size, semi-brittle flow and plastic yielding.

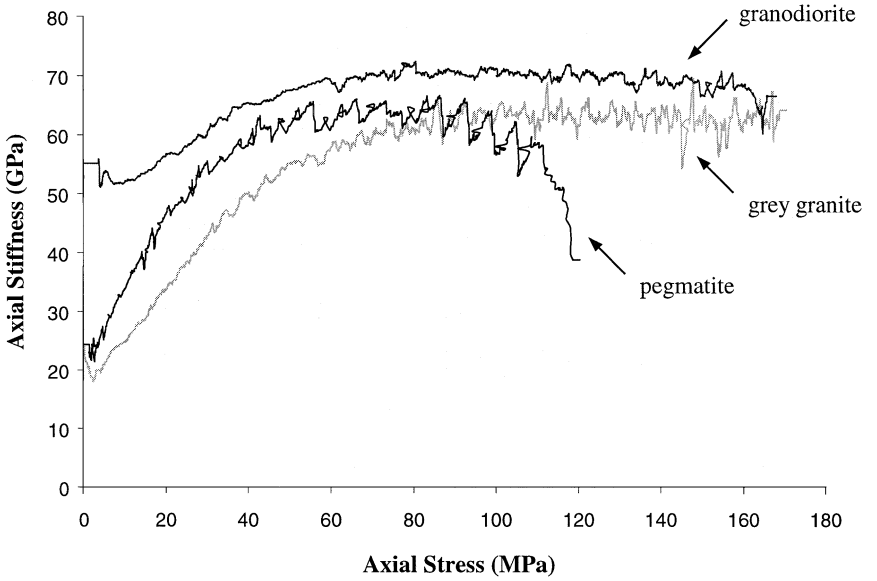

Fig. 5. Plots of axial stiffness *vs.* axial stress for URL 240 m level samples of granodiorite, grey granite and pegmatite

Examination of secant modulus values provided further insight into the relationship between grain size and stress-induced fracturing. The secant modulus, which includes the non-linearity in axial strain during initial loading and subsequent crack closure, can be used as an indicator of the initial crack volume in the sample prior to testing (e.g. "pre-existing" cracks induced during the sampling process or related to the *in situ* stress regime history). The larger the discrepancy between the secant and Young's modulus values, the greater the initial crack volume. Table 4 shows that the difference between secant and Young's modulus values for the granodiorite was less than 1%, and 22% and 14% for the grey granite and pegmatite respectively. Thus it would appear that the initial crack volume in the finer-grained granodiorite was much lower in relation to the coarser-grained grey granite and pegmatite.

Differences in the initial sample crack volumes were also discernable in plots of the axial stiffness. Stiffness plots are derived through a moving point regression analysis of the stress-strain curve and act to accentuate any deviations in the stress-strain behaviour of the rock (Eberhardt et al., 1998b). Initial axial stiffness values for the granodiorite were two to three times higher than those seen for the granite and pegmatite (Fig. 5). Crack closure was also achieved at lower stresses in the granodiorite than the grey granite (Table 5), confirming acoustic velocity tests which showed that the granite had a higher crack density (i.e. a high number of cracks per unit volume). Comparisons between the granodiorite and pegmatite values, however, reveal that the crack closure stresses were approximately the same. This would seem to suggest that the existing crack population in the pegmatite was relatively small in number, resulting in lower crack closure stresses, but

Table 5. Average crack thresholds for the 240 m level URL samples (standard deviation in parentheses)

Strength parameter	Granodiorite	Grey granite	Pegmatite
Number of tests	5	5	5
Crack closure, σ_{cc} (MPa)	45.6 ($\pm$3.4)	55.6 ($\pm$1.5)	45.2 ($\pm$2.7)
Crack initiation, σ_{ci} (MPa)	79.6 ($\pm$2.7)	79.6 ($\pm$2.3)	72.0 ($\pm$5.9)
Secondary cracking, σ_{ci2} (MPa)	102.8 ($\pm$4.5)	102.8 ($\pm$4.3)	96.0 ($\pm$4.4)
Crack coalescence, σ_{cs} (MPa)	164.7 ($\pm$9.0)	127.6 ($\pm$14.2)	104.8 ($\pm$6.4)
Crack damage, σ_{cd} (MPa)	194.0 ($\pm$2.8)	147.4 ($\pm$9.1)	113.2 ($\pm$6.8)

large in volume resulting in a low initial axial stiffness value. Both of these factors attest to the geometry of fewer but longer crack lengths that would be expected with larger grains and grain boundaries within the given sample volume.

The crack initiation, σ_{ci}, and secondary cracking, σ_{ci2}, thresholds for the granodiorite were the same as those for the grey granite (Table 5 and Fig. 6). This would seem to suggest that the initial stages of cracking are not strongly dependent on grain size, but are more related to the feldspar and quartz mineralogy. SEM observations by Eberhardt (1998) of thin sections taken from tested samples of pink Lac du Bonnet granite showed that the initial stages of detectable crack propagation are primarily intergranular as cracking begins (i.e. σ_{ci}) within the feldspar grains, followed by secondary cracking (i.e. σ_{ci2}) at higher loads within the quartz grains. These latter cracks appear to be generated through point load contacts, with grain boundary cracks playing a secondary role. A similar pattern was seen in the pegmatite with the exception that threshold values ($\sigma_{ci}, \sigma_{ci2}$) were approximately 10% lower than those seen in the granodiorite and granite. It should be noted, however, that these differences may be related to the size of the sample, relative to the maximum grain size. The difference in grain size between the granodiorite and grey granite, on the other hand, did not seem to influence significantly when intergranular microfracturing began.

Grain size did, however, affect the number of AE events recorded. Figure 7 shows that the number of detected AE events decreases markedly with decreasing grain size. The granodiorite produced approximately 90% fewer total AE events than the pegmatite, and 60% fewer total events than the grey granite. Accordingly, the grey granite produced approximately 60% fewer total events than the pegmatite. For all three rocks, a significant number of events were recorded during crack closure and prior to the crack initiation threshold, implying that such events are being produced through grain boundary movements.

SEM observations confirmed that, following crack initiation, σ_{ci}, an almost equal number of fractures originated within the feldspar grains at low stresses as along grain boundaries (Fig. 8). According to Griffith's theory larger grain boundaries critically aligned to the direction of loading should initiate before smaller ones. It then follows that the overall increase in the number of detected events with increasing grain size is due to the increasing number of cracks originating along grain boundaries. However, as previously noted, the grain size effect was seen to play a secondary role to the mineralogy in terms of the initial generation of propagating cracks.

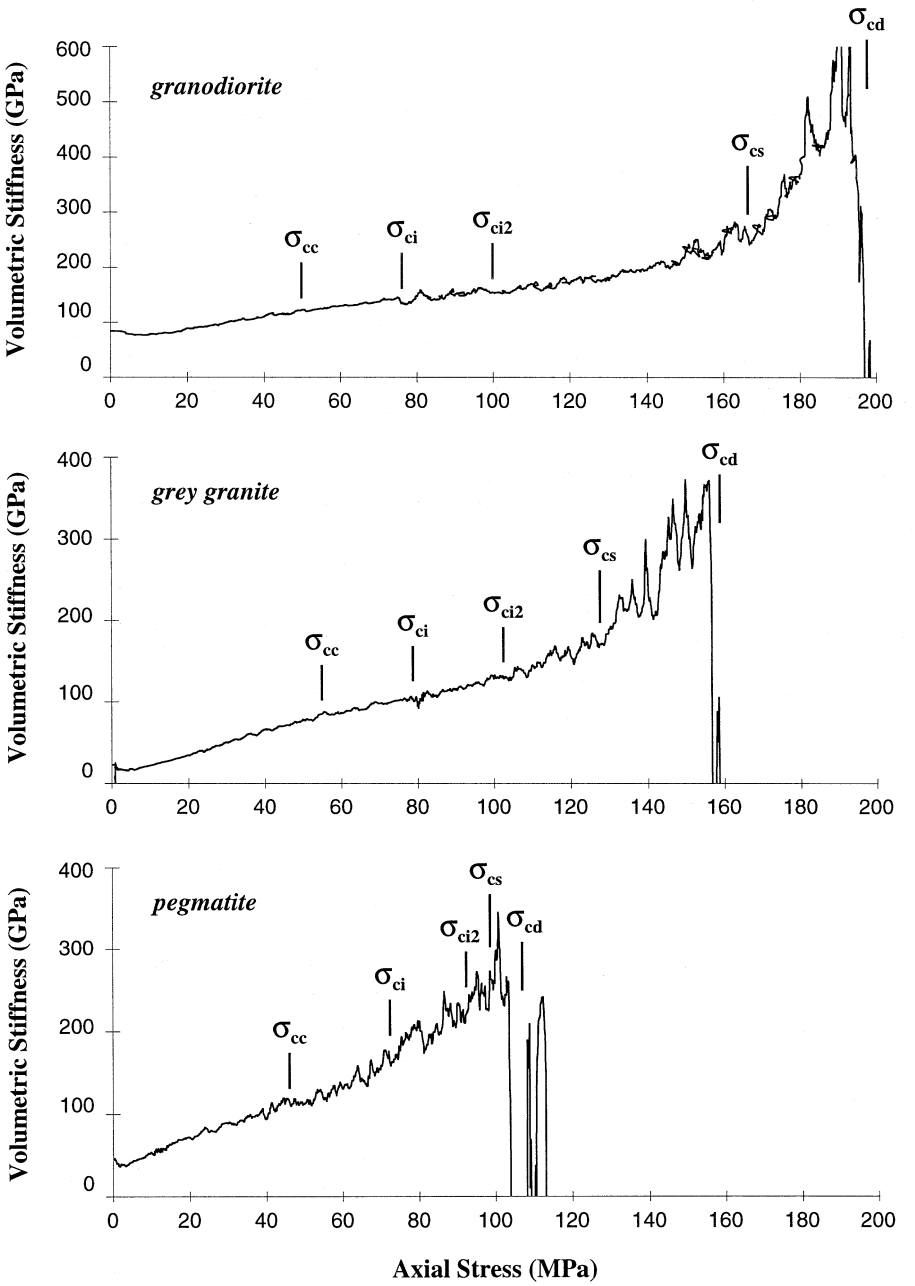

Fig. 6. Plots of volumetric stiffness *vs.* axial stress for URL 240 m level samples of granodiorite (top), grey granite (middle) and pegmatite (bottom)

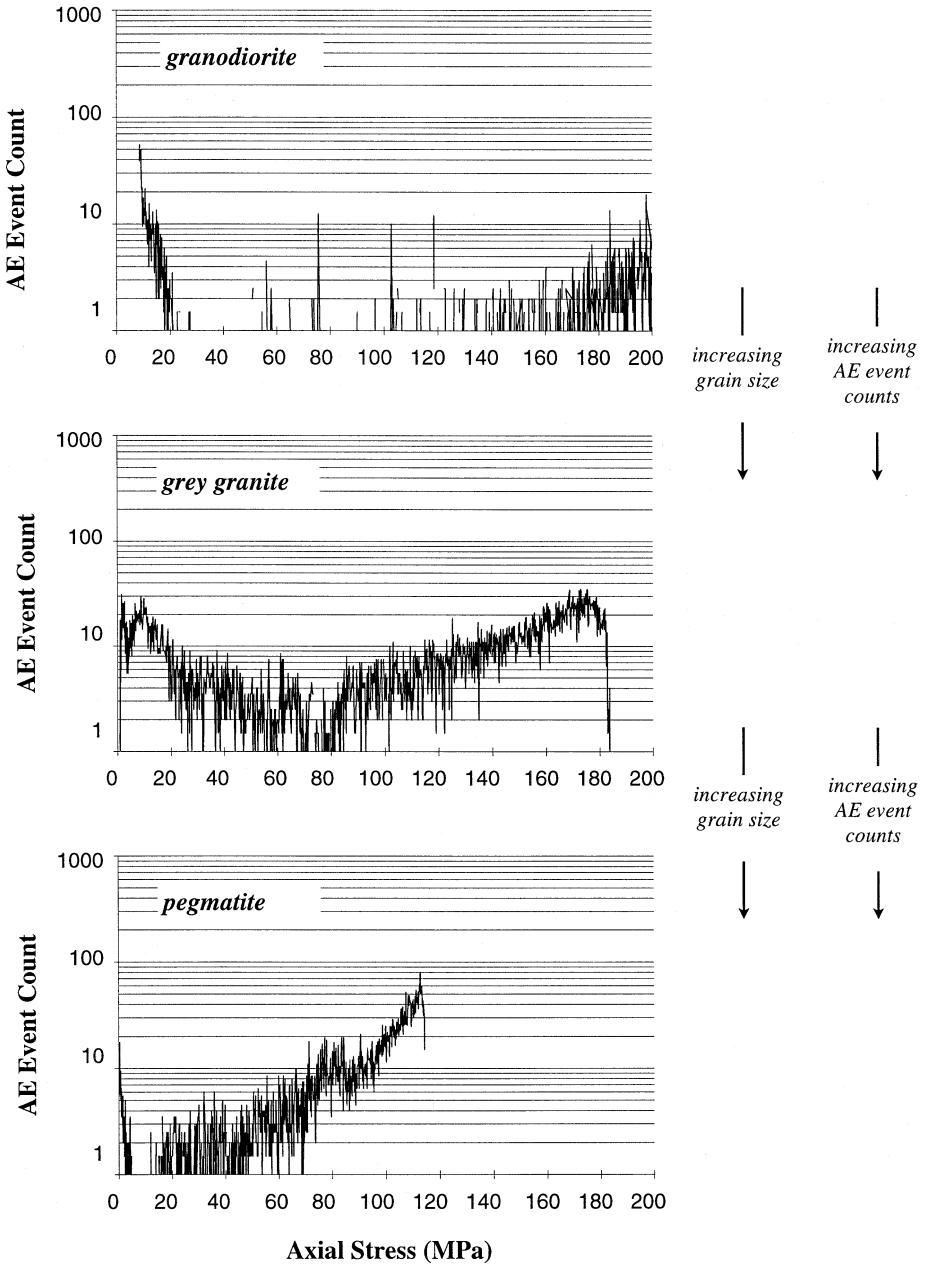

Fig. 7. Log plots of AE event count *vs.* axial stress for URL 240 m level samples of granodiorite (top), grey granite (middle) and pegmatite (bottom)

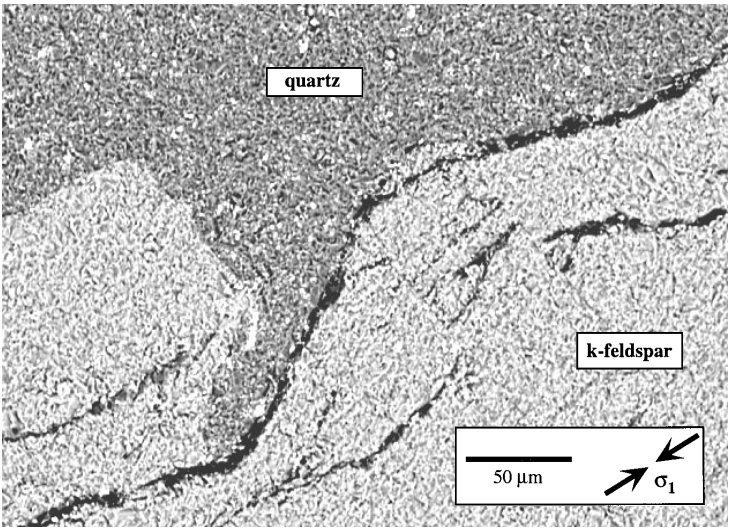

Fig. 8. SEM image of stress-induced cracks originating within a feldspar grain and along a quartz-feldspar grain boundary in a URL granite

The effects of grain size were seen to be most significant in terms of the crack coalescence, σ_{cs}, and crack damage, σ_{cd}, thresholds. Figure 6 and values in Table 5 show that the crack coalescence values for the grey granite and pegmatite decreased by 23% and 36%, respectively, when compared to values for the granodiorite. Values for the crack damage threshold decrease by 21% and 42%, respectively, when comparing grey granite and pegmatite values to the granodiorite. These results are in direct contrast to those for crack initiation, σ_{ci}, and secondary cracking, σ_{ci2}, thresholds which were relatively constant for all three rock types. In other words, grain size had minimal effects in terms of when intergranular cracking began, but the behaviour of the cracks during propagation was highly influenced by grain size.

Insight into crack behaviour following crack initiation may also be gained by examining plots of the calculated AE elastic impulse "energy" rate, which in turn, is based on the AE event's peak amplitude and duration (Eberhardt et al., 1998b). Figure 9 shows that event "energy" values for the granodiorite were relatively small when compared to values for the grey granite and pegmatite (it should be noted that these AE "energy" values are not absolute measures of energy, but can be used for comparative purposes). This provides valuable information with respect to the extent that the cracks are propagating. According to Griffith's criterion and the Griffith crack locus (Cook, 1965; Martin and Chandler, 1994), the amount of elastic energy released during crack propagation increases with increasing crack length extension (Fig. 10). AE event "energy" values in Fig. 9 suggest that crack propagation in the granodiorite is more limited, whereas significant propagation in the grey granite and pegmatite samples occurs, resulting in larger releases of kinetic energy. It would therefore appear that an important fac-

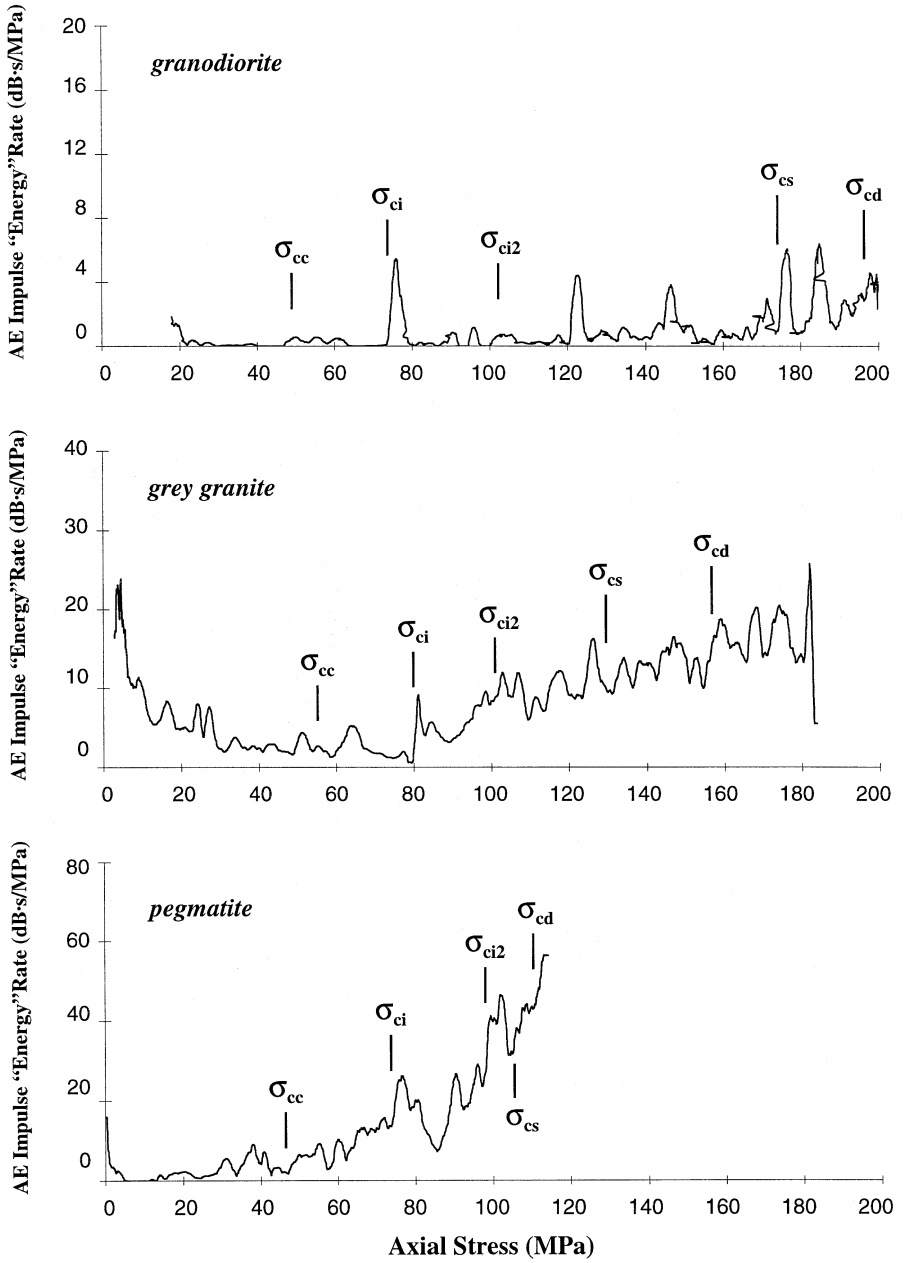

Fig. 9. Plots of the AE elastic impulse "energy" rate *vs.* axial stress for URL 240 m level samples of granodiorite (top), grey granite (middle) and pegmatite (bottom)

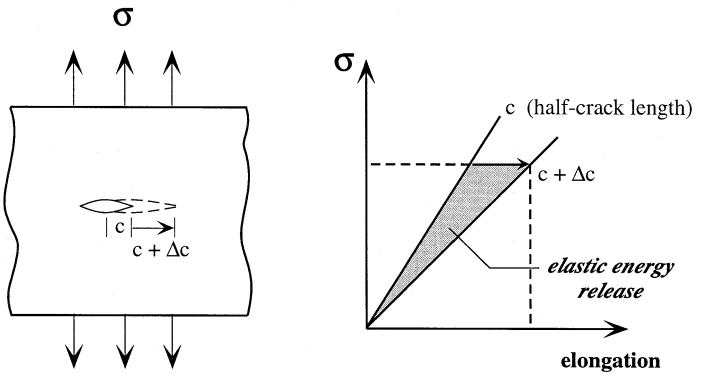

Fig. 10. The Griffith criterion, for a plate with fixed ends, showing the elastic energy released upon crack extension under constant load (after Broek, 1986)

tor responsible for limiting crack propagation is grain size. Numerical modelling results presented by Eberhardt et al. (1998a) have demonstrated that propagating cracks in close proximity to one another can interact in such a fashion as to inhibit crack propagation (e.g. crack arrest). These effects, as seen in the numerical models, diminished with increasing crack separation distances (i.e. increasing grain sizes). The lower crack coalescence and crack damage thresholds seen in the granite and pegmatite samples, may therefore be indicative of the reduced crack interaction due to larger distances (i.e. grain size) between cracks.

4. Summary and Conclusions

Uniaxial compression tests were performed to determine the effects of grain size on the development of stress-induced microfractures in crystalline rock. Samples of fine-grained granodiorite, medium-grained grey granite and coarse-grained pegmatite from the 240 m level of AECL's URL were used. A rigorous methodology, based on strain gauge and acoustic emission techniques, was developed and applied to the interpretation of the test results. The following observations and conclusions were made:

- An inverse relationship was found between grain size and acoustic velocity, Young's modulus and secant modulus. Conversely, higher velocity values were sometimes seen in the large-grained pegmatites in cases where large feldspar crystals dominated the sample.
- Analysis of the fracture threshold characteristics of the samples showed that grain size had relatively little influence on the crack initiation stress threshold. This was primarily due to the large number of cracks that initiated from within the feldspar and quartz grains as a result of point loading mechanisms. The development of these cracks was found to be more dependent on the strength of the constituent minerals than on their grain size. Grain size effects were seen to have a more significant influence on cracks originating along grain boundaries,

but were found to be minimal with respect to sample deformation and stiffness, although the number of detected AE events drastically increased with increasing grain size.

– Increasing grain size was found to reduce the crack coalescence and crack damage thresholds. It was reasoned that longer grain boundaries and larger intergranular cracks, due to increased grain size, provided more continuous paths of weakness for growing cracks to propagate along and promoted a more rapid degradation of material strength once these longer cracks began to coalesce and interact. Thus, rock strength was found to decrease with increasing grain size, not by inducing crack initiation sooner (as dictated by Griffith's empirical relationship), but through a process where cracks propagating along longer existing planes of weakness coalesce at lower stresses, resulting in failure at lower loads.

Acknowledgments

Parts of the work have been supported by Atomic Energy of Canada, Ltd. and a NSERC operating grant. The authors wish to thank Zig Szczepanik and Dr. Rod Read for their suggestions and contributions to this work. Special thanks are extended to Dr. Emery Lajtai and Dr. Derek Martin for their insights during the initial stages of this work.

References

Bieniawski, Z. T. (1967): Mechanism of brittle rock fracture: Part I – Theory of the fracture process. Int. J. Rock Mech. Min. Sci. Geomech. Abstr. 4 (4), 395–406.

Bombolakis, E. G. (1973): Study of the brittle fracture process under uniaxial compression. Tectonophysics 18, 231–248.

Brace, W. F. (1961): Dependence of fracture strength of rocks on grain size. Bulletin of the Mineral Industries Experiment Station, Mining Engineering Series. Rock Mech. 76, 99–103.

Brace, W. F. (1964): Brittle fracture of rocks. In: State of stress in the earth's crust: Proc., International Conference, Santa Monica, 110–178.

Brace, W. F., Silver, E., Hadley, K., Goetze, C. (1972): Cracks and pores: a closer look. Science 178 (4057), 162–164.

Broek, D. (1986): Elementary engineering fracture mechanics. Martinus Nijhoff Publ., Boston.

Brown, E. T. (1981): Rock characterization testing and monitoring: ISRM suggested methods. Pergamon Press, Oxford.

Cook, N. G. W. (1965): The failure of rock. Int. J. Rock Mech. Min. Sci. Geomech. Abstr. 2 (4), 389–403.

Eberhardt, E. (1998): Brittle rock fracture and progressive damage in uniaxial compression. Ph.D. thesis, Department of Geological Sciences, University of Saskatchewan, Saskatoon.

Eberhardt, E., Stead, D., Stimpson, B., Read, R. S. (1997): Changes in acoustic event properties with progressive fracture damage. Int. J. Rock Mech. Min. Sci. 34 (3/4), 633.

Eberhardt, E., Stead, D., Stimpson, B., Lajtai, E. Z. (1998a): The effect of neighbouring cracks on elliptical crack initiation and propagation in uniaxial and triaxial stress fields. Eng. Fracture Mech. 59 (2), 103–115.

Eberhardt, E., Stead, D., Stimpson, B., Read, R. S. (1998b): Identifying crack initiation and propagation thresholds in brittle rock. Can. Geotech. J. 35 (2), 222–233.

Fredrich, J. T., Evans, B., Wong, T.-F. (1990): Effect of grain size on brittle and semibrittle strength: Implications for micromechanical modelling of failure in compression. J. Geophys. Res. 95 (B7), 10907–10920.

Goodman, R. E. (1989): Introduction to rock mechanics. Wiley, New York.

Griffith, A. A. (1920): The phenomena of rupture and flow in solids. Philos. Trans. Roy. Soc. London, Series A, Math. Phys. Sci. 221 (587), 163–198.

Griffith, A. A. (1924): The theory of rupture. In: Proc., First International Congress for Applied Mechanics, Delft, 55–63.

Hatzor, Y. H., Palchik, V. (1997): The influence of grain size and porosity on crack initiation stress and critical flaw length in dolomites. Int. J. Rock Mech. Min. Sci. 34 (5), 805–816.

Hugman, R. H. H., Friedman, M. (1979): Effects of texture and composition on mechanical behavior of experimentally deformed carbonate rocks. The American Association of Petroleum Geologists Bulletin 63 (9), 1478–1489.

Kranz, R. L. (1979): Crack-crack and crack-pore interactions in stressed granite. Int. J. Rock Mech. Min. Sci. Geomech. Abstr. 16 (1), 37–47.

Kranz, R. L. (1983): Microcracks in rocks: a review. Tectonophysics 100 (1–3), 449–480.

Martin, C. D. (1993). Strength of massive Lac du Bonnet granite around underground openings. Ph.D. thesis, Department of Civil and Geological Engineering, University of Manitoba, Winnipeg.

Martin, C. D., Chandler, N. A. (1994): The progressive fracture of Lac du Bonnet granite. Int. J. Rock Mech. Min. Sci. Geomech. Abstr. 31 (6), 643–659.

Martin, C. D., Read, R. S., Martino, J. B. (1997): Observations of brittle failure around a circular test tunnel. Int. J. Rock Mech. Min. Sci. 34 (7), 1065–1073.

Mosher, S., Berger, R. L., Anderson, D. E. (1975): Fracturing characteristics of two granites. Rock Mech. 7 (3), 167–176.

Olsson, W. A. (1974): Grain size dependence of yield stress in marble. J. Geophys. Res. 79 (32), 4859–4862.

Read, R. S. (1994). Interpreting excavation-induced displacements around a tunnel in highly stressed granite. Ph.D. thesis, Department of Civil and Geological Engineering, University of Manitoba, Winnipeg.

Simmons, G., Richter, D. (1976): Microcracks in rocks. In: Strens, R. G. J. (ed.), The physics and chemistry of minerals and rocks. Wiley, Toronto, 105–137.

Sprunt, E. S., Brace, W. F. (1974): Direct observation of microcavities in crystalline rock. Int. J. Rock Mech. Min. Sci. Geomech. Abstr. 11 (4), 139–150.

Tapponnier, P., Brace, W. F. (1976): Development of stress-induced microcracks in Westerly granite. Int. J. Rock Mech. Min. Sci. Geomech. Abstr. 13 (4), 103–112.

Wawersik, W. R., Brace, W. F. (1971): Post-failure behavior of a granite and diabase. Rock Mech. 3(2), 5–85.

Wong, R. H. C., Chau, K. T., Wang, P. (1996): Microcracking and grain size effect in Yuen Long marbles. Int. J. Rock Mech. Min. Sci. Geomech. Abstr. 33 (5), 479–485.

Authors' address: Dr. Erik Eberhardt, Engineering Geology, ETH Hönggerberg, CH-8093 Zürich, Switzerland.